Supporting Information

Louis et al. 10.1073/pnas.1102278108

SI Materials and Methods

Small-Scale Cultures for Screening Inhibition of Protease Precursor Autoprocessing During Expression in *Escherichia coli*. Luria–Bertani medium (0.5–1 ml) containing 100 μg/mL of carbenicillin was prepared from a 2X stock with or without added PI to a final concentration of 8–150 μM (from 160 or 300 μM stock solutions of PIs). The medium was inoculated, to provide an initial optical density (OD) of 0.15 at 600 nm, with an overnight culture of *E. coli* BL-21 bearing the plasmid for the expression of the protease precursor. After incubation for approximately 100 min at 37 °C (OD of 0.6–0.7), protein expression was induced by the addition of 2 mM isopropylthiogalactoside for a period of 2 h. Cells were harvested, suspended in 0.3–0.4 ml 50 mM Tris-HCl, pH 8, 10 mM EDTA and 5 mM DTT (buffer A), and lysed by sonication (two cycles of 10–15 sec) in the presence of 100 μg/mL lysozyme. The insoluble fraction was recovered by centrifugation in an Eppendorf centrifuge spun at 12,800 rpm for 20 min at 4 °C. The pellet was suspended by brief sonication in 0.3 ml of 50 mM Tris-HCl, pH 8, 10 mM EDTA and 5 mM DTT containing 1 M urea and 0.5% Triton X-100 and recovered again by centrifugation. The final pellet was rinsed in buffer A and then dissolved in 15–30 μl of 8 M urea, 50 mM Tris-HCl, pH 8, 5 mM EDTA and 10 mM DTT. 5 μl of this protein solution was mixed with 2 μl of the SDS/PAGE sample buffer and subjected to electrophoresis on a 20% homogeneous PhastGel (GE Healthcare). Proteins were visualized by staining with PhastGel Blue R and band intensities were quantified using ImageJ software (rsb.info.nih.gov/ij/).

Differential Scanning Calorimetry. To avoid possible protein precipitation that was observed for TFR-PR_M at higher buffer concentrations, precursors were folded by addition of 5.66 volumes of 5 mM sodium acetate, pH 5.3, containing inhibitor, to 1 volume of precursor (approximately 2 mg/mL in 12 mM HCl) to give an approximately twofold excess of inhibitor to protein dimer and a final pH of approximately 5. Mature DRMs were folded as above (with or without inhibitor in the quench buffer) or by the two-step quench protocol as described previously (1) by addition of 2.33 volumes of 5 mM sodium acetate, pH 6 (with or without inhibitor) to one volume of protein solution, followed immediately by 3.33 volumes of 100 mM sodium acetate, pH 5.0. Final protein concentrations (as dimer) were 8–10 μM for the precursors and 13–14 μM for the mature enzymes. DSC scans on the MicroCal VP-DSC microcalorimeter were begun at 20 or 25 °C and run at a rate of 90 °C/h.

Isothermal Titration Calorimetry. ITC measurements of PI binding to mature PR mutants were performed in 50 mM sodium acetate buffer, pH 5, at 28 °C. Typically 6–10 μM folded (see above) protease in the sample cell was titrated with fifteen 2.45-μl injections of inhibitor at approximately 10 times the concentration of the protein. DMSO was added to the sample prior to titration to give the same concentration (typically ≤0.3% v/v) as that in the PI titrant solution. Data were analyzed by use of the Origin software provided with the MicroCal iTC_{200} instrument. Direct titration of $PR_{M\text{-}P51}$ with SQV gave a negligible thermal response on injection of the inhibitor into the protein solution, similar to that observed for titration of solvent alone. However, titration of $PR_{M\text{-}P51}$ with a relatively weak binder, RPB [H-Arg-Val-Leu-(r)-Phe-Glu-Ala-Nle-NH_2, where (*r*) represents a reduced (amine) peptide bond] exhibited a significant ΔH of approximately −5.4 Kcal/mol and a ligand-dissociation constant (K_L) of 0.8 μM. Consequently K_L for SQV was determined by displacement of RPB (added in a threefold molar excess relative to 6 μM $PR_{M\text{-}P51}$) by titration with 100 μM SQV. K_L for SQV (stronger binder) was calculated by use of the instrument's Origin software as well as by a simplified formula (2).

1. Ishima R, Torchia DA, Louis JM (2007) Mutational and structural studies aimed at characterizing the monomer of HIV-1 protease and its precursor. *J Biol Chem* 282:17190–17199.

2. Velazquez-Campoy A, Freire E (2006) Isothermal titration calorimetry to determine association constants for high-affinity ligands. *Nat Protoc* 1:186–191.

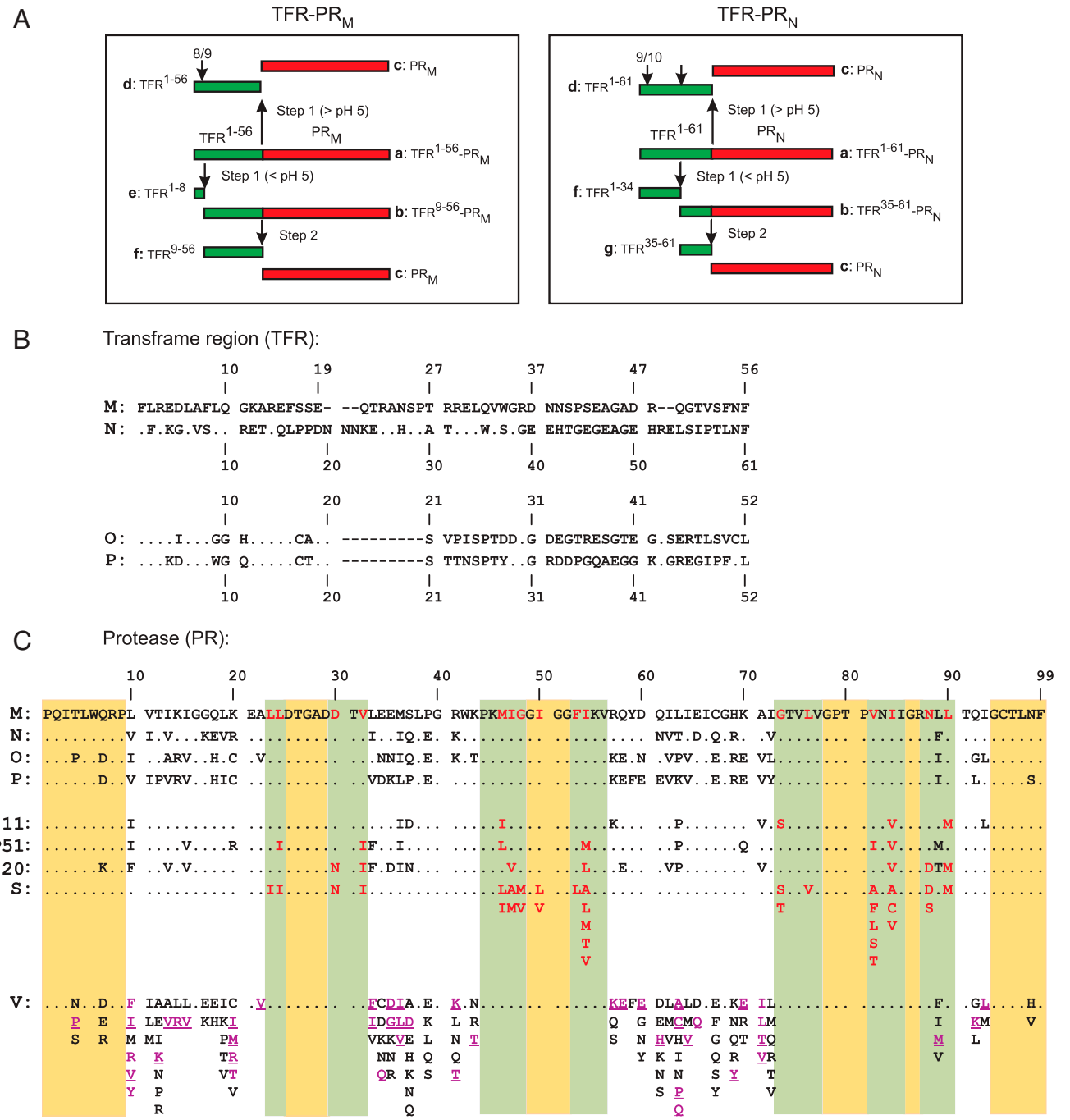

Fig. S1. (*A*) pH-dependent pathways for autoprocessing of TFR-PR$_M$ and TFR-PR$_N$. An initial cleavage step within the TFR (F8/L9 in group M (1) and L34/W35 in group N) (2) to give an intermediate lacking full catalytic activity, which is subsequently converted to the active mature protease by cleavage at the N terminus of the PR domain, is significant only at pH values <5 (downward arrows). Above pH 5, autoprocessing occurs mainly via a cleavage at the N terminus of the PR as the first step (upward arrows) concomitant with the appearance of stable dimer formation and mature-like catalytic activity (1, 2). Autoprocessing of the precursor in *E. coli* resembles the >pH 5 pathway with the predominant cleavage occurring at the N terminus of the PR as the first step. (*B*) Sequence alignment by ClustalW (Accelrys Gene) of the transframe regions of HIV-1 groups N (GenBank accession no. AY532635), O (AJ300450), and P (GQ328744) with group M. Consensus matches are indicated by dots. Note that the TFR of group N is the longest (61 amino acids). Dashes indicate residues not present in groups M, O, or P. The isolated TFR was shown to be mostly unstructured by solution NMR (3). The role of TFR in modulating protease function is not fully understood. It may mimic the role of a proregion, under specific conditions, similar to that seen with eukaryotic aspartic proteases such as pepsinogen conversion to pepsin (4). In spite of the sequence divergence, TFR-PR$_M$ and TFR-PR$_N$ precursors exhibit the same pattern and pH dependence for N-terminal autoprocessing as shown here schematically. Thus, sequence variations, except possibly for the cleavage sites within and at the C terminus of TFR (TFR/PR site), are not expected to influence the autoprocessing reaction or its inhibition significantly. Our kinetics and NMR studies indicate that the K_d of PR is significantly enhanced even by the addition of four residues flanking the N terminus of PR (C-terminal residues of TFR) (1, 5). In contrast, the flanking N-terminal reverse transcriptase residues at the C terminus of PR do not influence the K_d or the catalytic activity (1, 5). Even though in vitro viral replication is tolerant to large deletions and substitutions within TFR, a large nonnative sequence insertion was shown to interfere with maturation and virus production suggesting that the overall length of TFR may be critical for its function (6). (*C*) The wild-type PR sequence of group M (subtype B-HXB2) without Q7K, L33I, L63I, C67A, and C95A mutations optimized for biochemical and structural studies (5), is shown for alignment of proteases of natural variants of HIV-1 N, O, and P groups and three drug-resistant group M

mutants (DRMs). PR_{M-11}/virus 14/ANAM-11 (7, 8), PR_{M-P51} (protease 51P derived from a mixture of clinical isolates by selection in cell cultures grown with increasing concentrations of DRV) (9) and PR_{M-20} (10). Only the amino acid differences relative to PR_M are indicated for each group and DRM. The gold and white backgrounds indicate highly conserved regions in the protease domain as shown from studies of Ceccherini-Silberstein et al., (11) in drug treated patients and areas of greatest variability among isolates, respectively. Major DRM sites from the Stanford University HIV Drug Resistance Database (http:/hivdb.stanford.edu/cgi-bin/PIResiNote.cgi) are shown in red on green background. S lists all the major DRMs from the Stanford database. V lists all the natural variations and selected DRMs observed in PR_M (extracted from ref. 1) for the positions that vary in PR_N, PR_O and PR_P. In this list, natural variations in PR_M are listed alphabetically, selected DRMs are indicated in purple and residues common to both are underlined. Note there is very little overlap between the variable residues in different groups and major drug resistance sites.

1 Louis JM, Ishima R, Torchia DA, Weber IT (2007) HIV-1 protease: Structure, dynamics, and inhibition. *Adv Pharmacol* 55:261–298.
2 Sayer JM, Agniswamy J, Weber IT, Louis JM (2010) Autocatalytic maturation, physical/chemical properties, and crystal structure of group N HIV-1 protease: Relevance to drug resistance. *Protein Sci* 19:2055–2072.
3 Beissinger, et al. (1996) Sequence-specific resonance assignments of the 1H-NMR spectra and structural characterization in solution of the HIV-1 transframe protein p6. *Eur J Biochem* 237:383–392.
4 Louis JM, Wondrak EM, Kimmel AR, Wingfield PT, Nashed NT (1999) Proteolytic processing of HIV-1 protease precursor, kinetics and mechanism. *J Biol Chem* 274:23437–23442.
5 Louis JM, Weber IT, Tozser J, Clore GM, Gronenborn AM (2000) HIV-1 protease: Maturation, enzyme specificity, and drug resistance. *Adv Pharmacol* 49:111–146.
6 Leiherer A, Ludwig C, Wagner R (2009) Uncoupling human immunodeficiency virus type 1 Gag and Pol reading frames: Role of the transframe protein p6* in viral replication. *J Virol* 83:7210–7220.
7 Muzammil S, Ross P, Freire E (2003) A major role for a set of non-active site mutations in the development of HIV-1 protease drug resistance. *Biochemistry* 42:631–638.
8 Condra JH, et al. (2000) Drug resistance and predicted virologic responses to human immunodeficiency virus type 1 protease inhibitor therapy. *J Infect Dis* 182:758–765.
9 Koh Y, et al. (2010) In vitro selection of highly darunavir-resistant and replication-competent HIV-1 variants by using a mixture of clinical HIV-1 isolates resistant to multiple conventional protease inhibitors. *J Virol* 84:11961–11969.
10 Dierynck I, et al. (2007) Binding kinetics of darunavir to human immunodeficiency virus type 1 protease explain the potent antiviral activity and high genetic barrier. *J Virol* 81:13845–13851.
11 Ceccherini-Silberstein F, et al. (2004) Identification of the minimal conserved structure of HIV-1 protease in the presence and absence of drug pressure. *AIDS* 18:F11–F19.

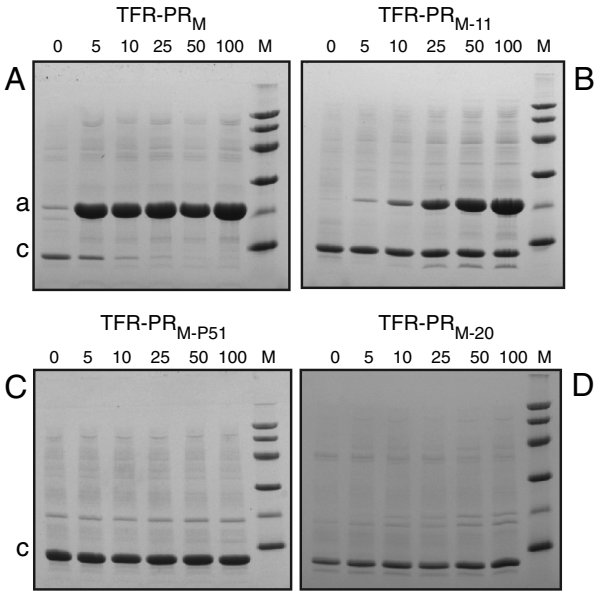

Fig. S2. Comparison of dose-response for inhibition of autoprocessing of PR_M and DRMs by DRV. The final concentration (μM) of DRV provided in the culture medium is indicated above the gels. M denotes standards as indicated in Fig. 3. Note that the total amount of precursor inhibition and accumulation varies among the constructs, with TFR-PR_M showing the maximum accumulation.

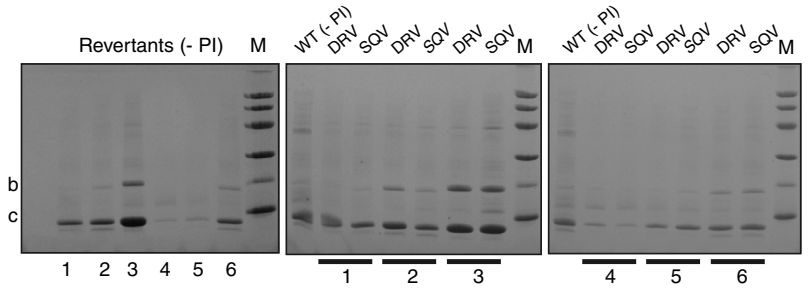

Fig. S3. Assessment of inhibition of autoprocessing of TFR-PR_{M-20} revertants by DRV. 1 ml cultures were grown either in the absence or presence of 100 μM DRV or SQV and induced for expression. Proteins were isolated as described, separated by SDS/PAGE, and stained. 1, 2, and 5 denote revertants bearing single mutations N30D, I32V, V84I, and 3, 4, and 6 denote revertants bearing double mutations N30D/I32V, V47I/L54I, D88N/M90L. WT (-PI) lane denotes wild-type TFR-PR_M precursor expressed in the absence of PI. TFR-PR_M shows maximum accumulation in the presence of 8–10 μM DRV or SQV with a IC_{50} of approximately 1 μM (Fig. 3*A*). Band intensities are comparable in the absence (*Left*) and presence of PI (*Middle* and *Right*) indicating absence of inhibition of autoprocessing both by DRV and SQV. Recently, DRMs were shown to modulate N-terminal autoprocessing such that a single L76V mutation, which significantly slows the rate of autoprocessing is compensated by a coselecting M46I mutation. Interestingly, during this selection, response to inhibition of autoprocessing also changes (1).

1 Louis JM et al. (2011) Drug resistance mutation L76V decreases the dimer stability and rate of autoprocessing of HIV-1 protease by reducing internal hydrophobic contacts. *Biochemistry* (in press).

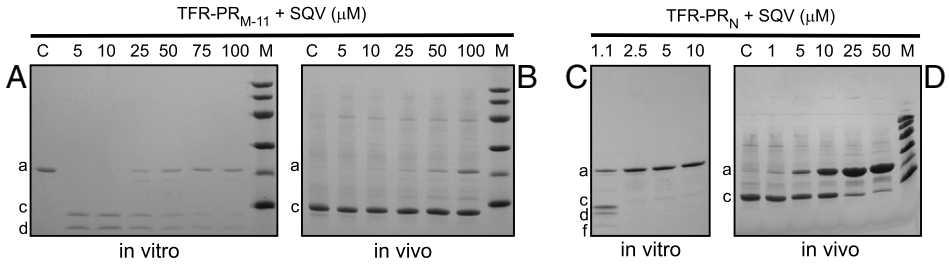

Fig. S4. Comparison of dose-response for inhibition of autoprocessing of TFR-PR_{M-11} (*A* and *B*) and TFR-PR_N (*C* and *D*) by SQV in vitro at pH 6.8 and in *E. coli* (in vivo). For in vitro processing, 1 volume of precursor in 12 mM HCl was folded by addition of 1.66 volumes of 5 mM sodium acetate buffer at pH 6 containing SQV, followed by 3.33 volumes of 40 mM sodium phosphate buffer, pH 7.1, to give final concentrations of 5 μM TFR-PR_{M-11} and TFR-PR_N and a pH of 6.8. Reactions were allowed to proceed at room temperature for 24 h. In vivo reactions followed the protocol described for monitoring autoprocessing in *E. coli* with the indicated concentrations of SQV in the culture medium. Samples were analyzed by SDS/PAGE either on 20% homogeneous PhastGels (*A*, *B*, *D*) or on 10–20% gradient Tris-Tricine gels (*C*).

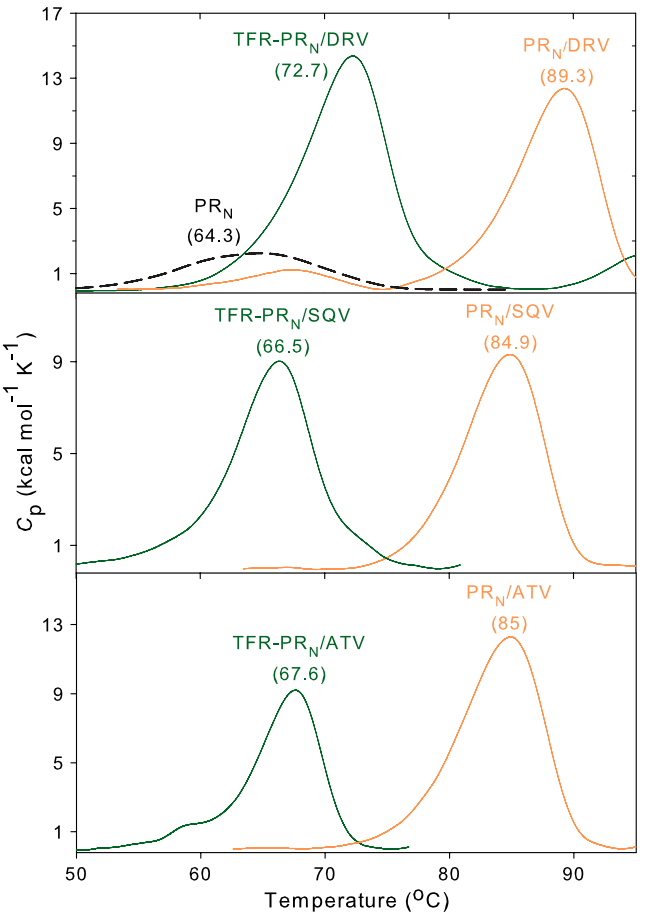

Fig. S5. Comparison of DSC thermograms of mature PR_N (1) and the precursor TFR-PR_N (this work) bound to a twofold excess of DRV, SQV, or ATV. Values of $T_{m.diff}$ are 16.6, 18.4, and 17.4 °C for TFR-PR_N bound to DRV, SQV, and ATV, respectively. Data for mature PR_N are reproduced from (1) for comparison with the precursor.

1 Sayer JM, Agniswamy J, Weber IT, Louis JM (2010) Autocatalytic maturation, physical/chemical properties, and crystal structure of group N HIV-1 protease: Relevance to drug resistance. *Protein Sci* 19:2055–2072.

Table S1. Kinetic parameters and dimer dissociation constants of mature wild-type and DRM proteases

Construct	k_{cat} (min^{-1})	K_m (μM)	k_{cat}/K_m (μM^{-1} min^{-1})	K_d (μM)
PR_M*,†	173 ± 2.9	48 ± 3	3.6 ± 0.3*	<0.01†
PR_N‡	170 ± 4	25 ± 3	6.8 ± 1	0.15 ± 0.06
PR_{M-11}	§	§	§	0.10 ± 0.04
PR_{M-P51}	60 ± 4	354 ± 43	0.17 ± 0.03	<0.1
PR_{M-20}	215 ± 19	617 ± 84	0.35 ± 0.08	0.029 ± 0.01

*Ref. 1.
†Ref. 2.
‡Ref. 3.
§K_{cat} is 3.8 times larger, and K_m is 2.1 times larger for PR_{M-11} (4) relative to wild-type PR_M under the same conditions; thus K_{cat}/K_m is 1.8 times larger for PR_{M-11} than for PR_M.

1 Ishima R, Torchia DA, Lynch SM, Gronenborn AM, Louis JM (2003) Solution structure of the mature HIV-1 protease monomer: Insight into the tertiary fold and stability of a precursor. *J Biol Chem* 278:43311-43319.
2 Louis JM, Clore GM, Gronenborn AM (1999) Autoprocessing of HIV-1 protease is tightly coupled to protein folding. *Nat Struct Biol* 6:868–875.
3 Sayer JM, Agniswamy J, Weber IT, Louis JM (2010) Autocatalytic maturation, physical/chemical properties, and crystal structure of group N HIV-1 protease: Relevance to drug resistance. *Protein Sci* 19:2055–2072.
4 Muzammil S, Ross P, Freire E (2003) A major role for a set of non-active site mutations in the development of HIV-1 protease drug resistance. *Biochemistry* 42:631–638.

Table S2. DSC data for inhibitor binding to mature wild-type and DRM proteases and their precursors

Construct	T_m, PR (°C)	T_m, PR + DRV (°C)	ΔT_m (°C)	T_m, Precursor + DRV (°C)	$T_{m.diff}$ (°C)
PR_M*/TFR-PR_M	65.7	88.1	22.4	66.7	21.4
PR_N[†]/TFR-PR_N	64.3	89.3	25	72.7	16.6
PR_{M-11}/TFR-PR_{M-11}	70.5	81.9	11.4	nd	nd
PR_{M-P51}[‡]/TFR-PR_{M-P51}	58.2	70.9	12.7	nd	nd
PR_{M-20}/TFR-PR_{M-20}	71.7	77.0	5.3	nd	nd

*Ref. 1.

[†]Ref. 2.

[‡]PR_{M-P51} shows a T_m of 71.3 °C in the presence of SQV; thus, a ΔT_m of 13.1 °C as compared to 12.7 °C observed with DRV.

nd denotes not determined, either because of very poor thermal response (TFR-PR_{M-11}) or unavailability of the precursor because of no precursor accumulation (TFR-PR_{M-20} and TFR-PR_{M-P51}) when grown in the presence of PI.

1 Sayer JM, Liu F, Ishima R, Weber IT, Louis JM (2008) Effect of the active-site D25N mutation on the structure, stability and ligand binding of the mature HIV-1 protease. *J Biol Chem* 283:13459–13470.

2 Sayer JM, Agniswamy J, Weber IT, Louis JM (2010) Autocatalytic maturation, physical/chemical properties, and crystal structure of group N HIV-1 protease: Relevance to drug resistance. *Protein Sci* 19:2055–2072.